Development of a Lightweight Fume Hood for Handheld Welding Guns

The hood has the ability to capture fumes at the source, reduce required suction flow rates, and provide shielding against UV radiation and spark exposures

BY NEDIM TURKEM, HARUN BILIRGEN, GUILLERMO A. VIECCO, AND HUGO S. CARAM

ABSTRACT. A small welding hood that completely covers the welding area was used to minimize welding fume emissions and the volume of gas treated. Very small volumetric flows (2 ft^3/min vs. 50 ft^3/min in a high-vacuum system) were required to completely eliminate measurable fume emissions. Preliminary data also indicate a reduction of up to 50% in the shield gas consumption. A low-cost vision system was also developed to guide the welding process. The hood also greatly reduces, or eliminates, UV exposure, spattering, and noise.

Introduction

Welding processes generate fumes that are hazardous to the health of the welder. Of these components, iron oxide (Fe_3O_4), ozone (O_3), and nitrogen oxides (NO, NO_2) cause eye, throat, and lung irritation, and possible long-term effects. In stainless steel welding, chromium, when present in hexavalent state (Cr^{VI}), is of particular concern to researchers since it is a cancer-causing agent and a mutagen in humans. Also present in stainless steel fumes and a cause of concern are nickel (Ni), another carcinogen that may also damage a developing fetus, and manganese (Mn), which may cause gradual brain damage with repeated exposure. Moreover, epidemiological studies and case reports of workers have revealed (Refs. 1–3) that welders, as an occupational group, suffer more acute and chronic respiratory ill-health effects than the general public (Ref. 1). Therefore, the control of occupational exposure to welding fumes continues to be a major problem for health and safety in the workplace.

The Occupational Safety and Health Administration (OSHA) has been evaluating the effects of occupational exposures to Cr^{VI} and Mn in anticipation of reducing the current Permissible Exposure Levels (PEL). The American Conference of Governmental Industrial Hygienists (ACGIH) reduced the Threshold Limit Value (TLV) of Ni, which is likely to impact the OSHA PEL evaluation. Current and anticipated OSHA regulation limits for worker exposure to welding fume components are tabulated in Table 1 (Ref. 4).

Compliance with these more stringent exposure standards using conventional welding fume collection techniques will have an economic impact on the operations and costs in, among others, the marine services industry (Refs. 5, 6). According to final rule OSHA PEL, either existing fume control methods have to be improved or, new efficient and cost-effective welding techniques must be developed. Most of the published research has been directed to improving the existing welding techniques, preventing the production of welding fumes by changing the chemical composition of the filler rod, or switching to other welding methods (Ref. 7).

A more efficient way of eliminating welding fumes might rely on the idea of controlling the fume at the source since the volume of the gas fumes to be removed increases rapidly as the fume-removal device moves away from the welding spot because of the dilution of the plume. To avoid the dilution, this study investigates a hood that completely covers the welding gun. Several hood design options were developed and tested in flux cored arc welding (FCAW) and gas metal arc welding (GMAW) of mild steel and stainless steel (AL-6XN) with an IN-622 electrode. The hood design that gave the best results is presented. Since the hood completely covers the welding area, a miniature CCD camera is fit to the hood to guide the welding process. Development of an inexpensive, reliable vision system was an important part of the project. Additional advantages with the use of the hood were the elimination of UV exposure, spattering, and a reduction in the amount of shielding gas. These advantages make the hood very attractive and overcome its drawbacks such as the small additional weight to the welding gun and the need for a television monitor or a head up display. Finally, it makes it possible to record the weling process for future reference.

KEYWORDS

Hood
Welding Gun
Fume
CCD Camera
FCAW
Weld Pool
Plume

Conventional Welding Fume Collecting Devices

The dispersion of the fume into the environment is significantly enhanced by the use of shielding gases, common in most welding processes. As a result of dispersion processes and buoyancy, fumes rise rapidly and occupy a large volume. For this reason, the volume to be treated may be thousands of times greater than the amount of fumes produced by the welding process. It is also necessary to separate the fine metal particles, which are formed as a result of condensation and the oxidation process during arc welding from the ventilation air. A fine filter element must be used to collect these submicron metal particles having diameters of approximately 0.25 μm (Ref. 8). Therefore, the welding fume-collecting systems have to be built separately from the regular ventilation systems (Ref. 9). Many different types of fume-collecting devices and systems for welding have been developed. These devices can be divided in two main groups: low- and high-vacuum systems.

Low-vacuum fume-collecting units have large suction flow rates, typically between 600 and 900 ft^3/min (17.0 and 25.5 m^3/min), at low velocity and pressures of 3–5 inches of water gauge. In these devices, a nozzle is placed near the weld (i.e., 0.6 m), and it is connected to a filter unit with a hose arm. The hose arm is flexible and can be easily repositioned. The suction flow rate of a nozzle can be up to 25,000 g/min, while in most cases the welding fume formation rate is about 1 g/min (Ref. 10). Low-vacuum collecting devices

NEDIM TURKEM, HARUN BILIRGEN, GUILLERMO A. VIECCO, and HUGO S. CARAM are with Lehigh University, Chemical Engineering Department, Bethlehem, Pa.

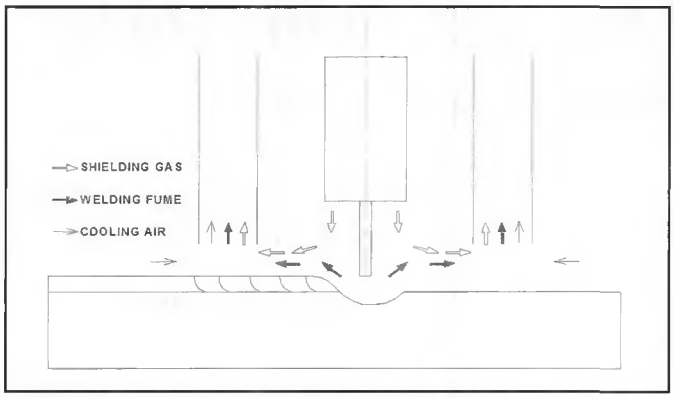

Fig. 1 — Desired flow patterns in the vicinity of the handheld welding hood.

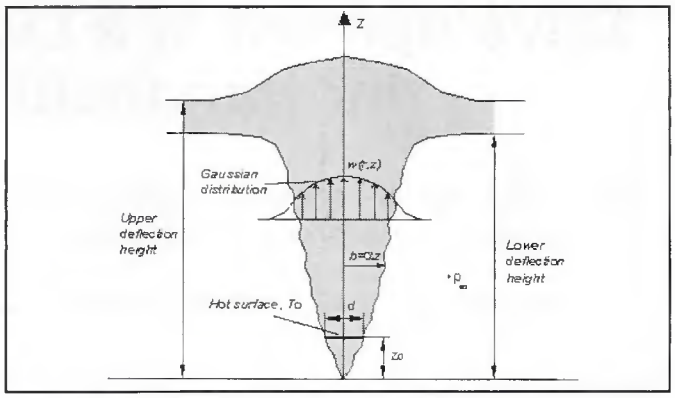

Fig. 2 — Theoretical model for plume flow.

Table 1 — OSHA PEL for Some Components of Stainless Steel Weld Fume

Fume Component	Current PEL (mg/m^3)	Anticipated PEL (mg/m^3)
Cr^{VI}, chromium chromates	100	100
Mn, metal and insoluble compounds	5000	1000
Ni, metal and insoluble compounds	1000	100

can be mounted on a wall or can be made into a portable unit that includes a filter and a suction device. In some cases, a suction unit can be connected to a main system with more than one collecting arm.

High-vacuum fume-collecting units have relatively low flow rates, between 35 and 150 ft^3/min (1 and 4.25 m^3/min), at pressures of 45–70 inches of water gauge. High-vacuum systems are mounted either directly on the welding gun or very close to it (i.e., 0.1 m), thus allowing fume control using much lower suction flow rates. A typical high-vacuum device has a volumetric flow rate of 50 ft^3/min (1.41 m^3/min) for a single welding gun (Ref. 11). Although various combinations of these ventilation systems have been used in the welding industry, the control of occupational exposure to welding fumes continues to be a major problem. Because of the high-suction flow rates, low-vacuum devices require large suction units and filter elements. Most of them are mounted on the wall and working distances are limited. The collection arms of these devices must be repositioned frequently, which is not done in practice. The position of the suction nozzle is very important for the welding quality in high-vacuum systems. The nozzle must be positioned a certain distance away from the welding point so that the suction flow does not disturb the shielding gas distribution on the welding pool. Therefore, the major challenge in this system is to maintain the welding quality. If the suction flow rate through the nozzle is high, it disturbs the shielding gas distribution and deteriorates the welding quality. Therefore, it is required that the welder fine-tune the exhaust flow rate for each setup.

Fume Hood Design for a Handheld Welding Gun

There are some considerations in designing a hood for a handheld welding gun. First, the hood should be small and not bulky. Second, the suction from the hood should not disturb the shielding gas distribution over the weld pool. Possible hood designs should ensure the flow patterns shown in Fig. 1. This pattern can only be achieved if the hood completely covers the arc and the weld pool. If this is the case, a camera system must be coupled to the hood in order to observe the welding as it is carried out. The welding process is then observed on a television screen. Also, if the hood completely covers the weld pool, cooling must be provided to the hood. In order to obtain a successful design, a mathematical model of the welding plume fume was developed to determine the suction flow rate required to completely remove the fume. An economical vision system was developed so that complete coverage of the welding pool could be obtained while viewing the welding process.

The Welding Fume Plume

In electric arc welding processes such as GMAW, the arc creates a plasma with temperatures ranging from 3000 to 10,000 K (Ref. 7). At these temperatures, the metals in the electrode are melted, and depending on their vapor pressures, some portion of the metals evaporates (Ref. 12). The hot vapors and the shielding gas rise upward to form a plume and, for a brief instant, are present as a metal vapor before condensing in the cooler air to form a fume aerosol having particle diameters less than 0.5 μm (Ref. 13). The weld fume is dissipated upward by the thermal air currents above the molten weld and may subsequently enter the breathing zone of the welder (Ref. 8). Velocities of weld fume plume in the neighborhood of the welding point can be as high as 1 m/s due to the large density differences between fume and surrounding air. Since fume dispersion is driven by natural convection, the flow rate in the plume depends on the energy losses to the air. As the plume rises, it entrains surrounding gas and the contaminants are diluted. Eventually, the density of the welding fume approaches the density of the surrounding air, and the plume stops its upward movement at the upper deflection point. At this point, the weld fume diffuses sideways. Also important is that vaporized metal nucleates and condenses into a very fine aerosol, where the very active fine metal particles also react with the surrounding atmosphere and are oxidized, constituting another contamination source.

The high temperature in the arc region causes large density differences that induce a turbulent thermal plume that carries the fumes upward. Since the design parameters of any welding hood and suction unit depend on the flow characteristics of the fume plume and fume-generation rates in the arc welding, calculations of welding fumes were performed assuming a turbulent axisymmetric buoyant flow created by a small surface with a very high temperature. A sketch of the plume flow considered in this study is given in Fig. 2.

Recent studies on turbulent buoyant

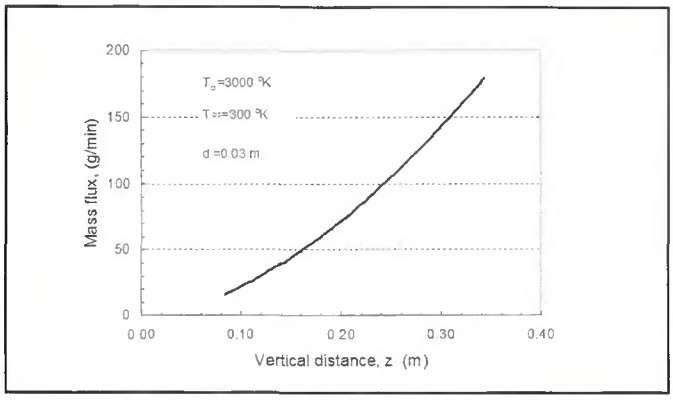

Fig. 3 — The variation of the plume mass flux for the case of the pure air.

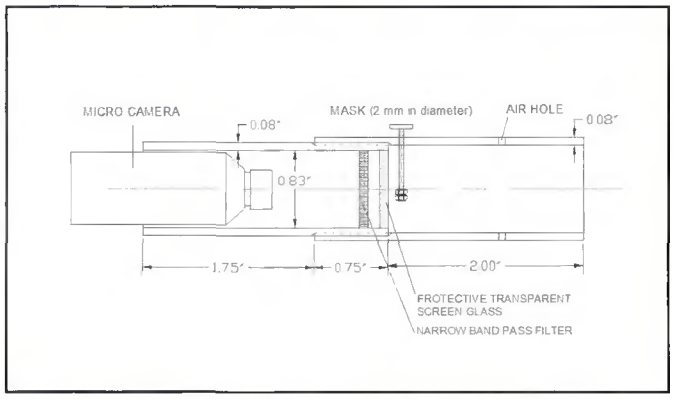

Fig. 4 — Scheme of the welding vision system using a CCD camera.

plumes have been performed by George et al. (Ref. 14), Malin (Ref. 15), and Dewan et al. (Ref. 16). List (Ref. 17) has defined the buoyancy flux of the thermal plume by volumetric expansion of fluid as

$$F_o = \frac{gQ_o}{c_p \rho_0 T_0} \qquad (1)$$

where Q_o is the heat flux at $z = z_o$, given by

$$Q_o = \frac{\pi d^2}{4} h(T_o - T_\infty)$$

c_p is the specific heat of the fluid, and T_0 is the temperature of the source. Notice that the correlations assume that at $z = 0$ the buoyancy source is a point source, while the actual source is distributed over a finite area of diameter d_0 and $z_0 = \alpha d_0$.

The velocity profile (w) and buoyancy distribution (g') for the case of axisymmetric plume were obtained experimentally by Rouse et al. (Ref. 18) and given as

$$w = k_1 F_o^{1/3} z^{-1/3} \exp(-e_1 r^2 / z^2) \qquad (2)$$

$$g' = g\frac{\Delta\rho}{\rho_\infty} = k_2 F_o^{2/3} z^{-5/3} exp(-e_2 r^2 / z^2) \qquad (3)$$

where $k_1 = 4.7$, $e_1 = 96$, $k_2 = 11$, $e_2 = 71$, and $\alpha = 0.18$.

From Equation 3, the density distribution in the plume can be obtained as,

$$\rho = \rho_\infty (1 - \frac{g'}{g}) = \rho_\infty (1 - \frac{k_2 F_o^{2/3} z^{-5/3} \exp(-e_2 r^2 / z^2)}{g}) \qquad (4)$$

The total mass flux at any distance from the welding point can be calculated by

$$m = 2\pi \int_0^b \overline{w} \rho r dr \qquad (5)$$

Integration of Equation 5 yields

$$m = \rho_\infty \pi \left[\frac{k_1 F_o^{1/3} z^{5/3} (1 - e^{(-\alpha^2 e_1)})}{e_1} - \frac{k_2 F_o (1 - e^{(-\alpha^2 (e_1 + e_2))})}{g(e_1 + e_2)} \right] \qquad (6)$$

Since

$$e^{(-\alpha^2 e_1)} << 1$$

and

$$e^{(-\alpha^2 (e_1 + e_2))} << 1,$$

these terms can be neglected. Therefore, Equation 6 can be expressed as

$$m = \rho_\infty \pi \left[\frac{k_1 F_o^{1/3} z^{5/3}}{e_1} - \frac{k_2 F_o}{g(e_1 + e_2)} \right] \qquad (7)$$

The second term in Equation 7 is small

Fig. 5 — View of the arc and weld pool using a CCD camera with a narrow-band-pass filter and an optical mask (arc is on).

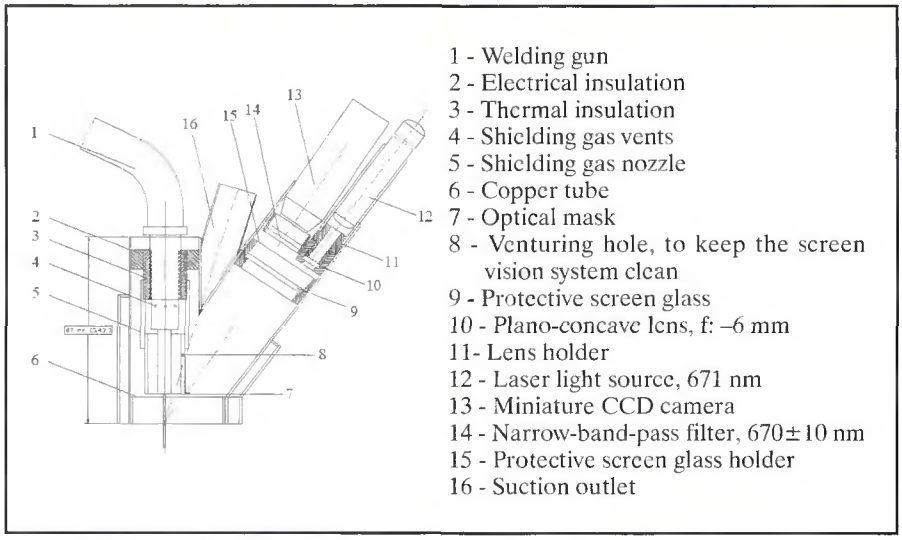

Fig. 6 — Lightweight fume hood design for the handheld welding gun.

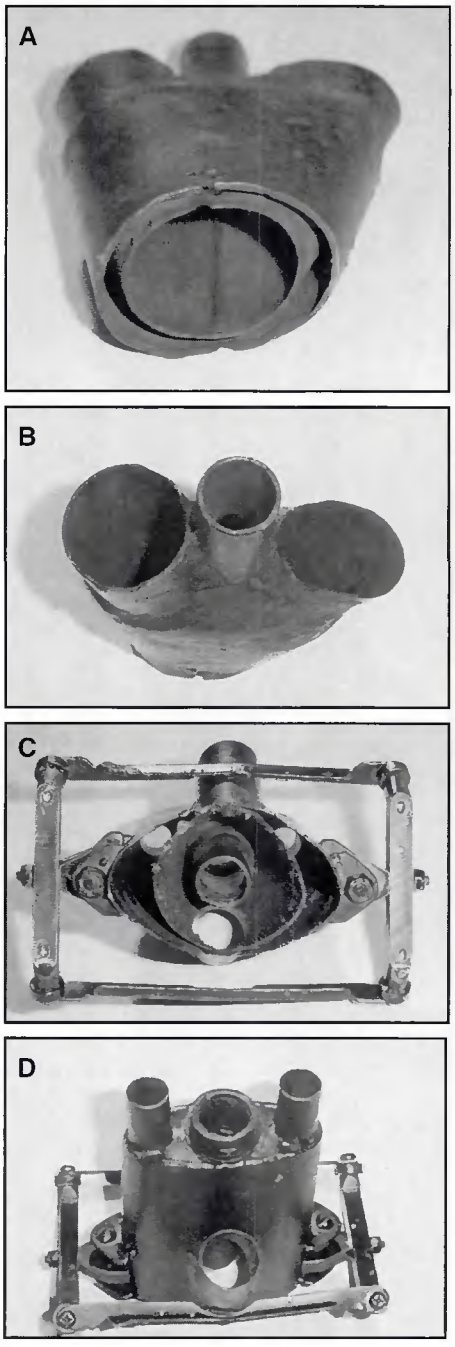

Fig. 7 — Lightweight fume hoods for the handheld welding gun. A — Hood for flat surface welding, bottom view; B — hood for flat surface welding, top view; C — hood for exterior 90-deg corner welding, bottom view; D — hood for interior 90-deg corner welding, top view.

in comparison with the first term since $F_o << 1$. Thus, the final form of the mass flux equation becomes

$$m = \frac{\rho_\infty \pi k_1 F_o^{1/3} z^{5/3}}{e_1} \qquad (8)$$

According to Equation 8, the mass flux

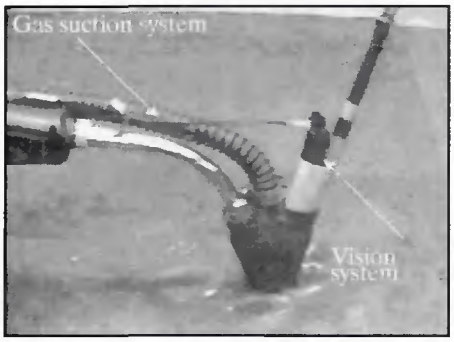

Fig. 8 — The lightweight hood for a flat surface mounted on a Magnum 400 welding gun. The gas suction and vision system can be seen.

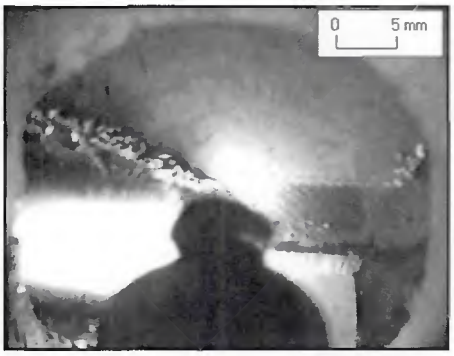

Fig. 9 — View of the welding process inside the lightweight hood using the CCD camera (the arc is on). The light region to the left is the weld pool, while the dark region at the center bottom corresponds to the mask. The gap between the pieces being joined is to the right. The light grey regions surrounding the image are the hood walls.

is proportional to $z^{5/3}$. This equation suggests that even in very short distances from the source, the mass flux rapidly increases. For instance, the mass flux increases more than 100 times at a distance 0.15 m (z_o = 8.3 cm) of the source. If the heat flux can be calculated at z_o, the buoyancy flux and the mass flux can be obtained at any point z. The heat flux at the beginning can be calculated using the Nusselt number derived for air on a horizontal plate. The average Nusselt number is given by Fishenden and Saunders (Ref. 19) as

$$Nu = 0.54(Gr\,Pr)^{1/4}, \quad 10^5 < (Gr\,Pr) < 10^7 \qquad (9)$$

The mass flux of the plume can be calculated using Equations 1, 8, and 9 as a function of distance from the welding point. The geometry of the welding area can be assumed to be circular, having a diameter of 0.03 m and temperature of 3000 K. Figure 3 illustrates the plume mass flow rates as a function of vertical distance, z. This provides a strong justification for the use of a localized hood.

Effect of Metal Condensation

The welding plume may contain a variety of components, depending on the electrode composition. Initial particle formation is a complex process. As the plume rises, fine particles are formed as a result of condensation of metal vapors and coagulation of the condensed particles. In very short distances, the vapor concentration is depleted by condensation. After this point, the plume consists of only a mixture of the fine particles and air. Particulate buoyant plumes were studied by Baum and Mulholland (Ref. 20), and the effect of the particles was taken into account by an additional term to the buoyancy equation

$$g' = g\left(\frac{\Delta\rho}{\rho_\infty} - x\right) \qquad (10)$$

where x is the particulate mass fraction (*kg-particle/kg-air*).

Comparison of Equation 10 with Equation 3 reveals that the particles in the plume mixture reduce the buoyancy and, therefore, the buoyancy flux calculated in Equation 5. This requires that the mass flow rates decrease since it is proportional to F_o (Equation 1). Therefore, the mass flow rates of the welding fumes in the presence of particles will always be lower than for the case of plume of pure air.

The FCAW process is known to generate the highest fume rates (0.5 to 2.5 g/min) compared to other welding techniques (0.0 to 0.7 g/min) (Ref. 21). According to the maximum fume-generation rates and the mass flow rates of the pure air calculated in Fig. 3, the particle mass fraction, x, at the beginning, z_o, can be calculated as 0.125. This value is relatively small in comparison with the term, $\varnothing\rho/\rho^\circ$, in Equation 10, which is approximately 0.9. Therefore, the pure air assumption for flow rate calculations is reasonable.

Hood design calculations were performed according to the maximum plume mass flux rates, which were based on the pure air assumption. The height of the hood determined the mass flux to be exhausted by the suction unit as is given by Fig. 3. After choosing the height, the mass flux and the volumetric flux of the plume, which determines the capacity of the suction unit, were calculated.

Vision System for the Welding Hood

Since the welding area is completely covered by the hood, a viewing system is necessary for the welders to see the welding pool. Monitoring of the arc welding process using a video camera is very diffi-

cult because of the variations in light intensity. The arc itself is extremely bright and floods the camera sensors so that the surrounding details cannot be observed. Several techniques have been developed to view the arc and the weld pool (Refs. 22–25). These are

a) *High-intensity illumination system*. A high-intensity light source is combined with very short exposure time to illuminate the weld pool to reduce the differences in the intensities in the arc area. This also reduces the dynamic range of arc light so that the camera sensor detects the images.

b) *High-quality laser source with an interference filter*. High-quality lasers such as He-Ne or Ar lasers produce a nearly monochromatic light. When an appropriate interference filter is used, most of the arc light can be eliminated because the filter only permits the laser light to pass through. As result, the vicinity of the arc can be viewed clearly.

c) *Pulsed laser in pulsed arc welding processes and synchronizing the laser to the welding machine*. This technique can only be used in pulsed welding processes and is very expensive.

Although high-quality arc images can be obtained by using some of the methods described above, they are expensive and bulky, which makes them impossible to use with the present hood design. Instead, a new viewing technique, which consisted of a miniature CCD camera, a laser, a narrow-band-pass filter, and an optical mask was developed to see and record the images from the weld pool enclosed by the hood.

A miniature black-and-white CCD camera (Model No. V-1212-BNC) by Marshall Electronics, California (Ref. 26), is used. A 12-mm focal length lens is used to view only the weld pool area. In order to reduce the light intensity of the arc, a narrow-band-pass filter is used. The filter permitted only the light with a wavelength of 671 nm (Full-Width Half-Maximum, FWHM=10 nm) to pass through. A protective transparent screen glass is mounted in front of the filter to protect the filter and the CCD camera system from arc sparks. In order to keep the visualization and illumination windows clean, some air is allowed to enter through holes drilled on the supporting tubes. To illuminate the region while the arc is off while still using a narrow-band-pass filter in the camera, a low-cost 5-mW laser pointer is used as an illumination source, having a wavelength of 670 nm (±10 nm). In order to illuminate the whole weld pool area, the laser beam is expanded by the use of a plano-concave lens, which has a focal length and a diameter of –6 and 6 mm, respectively.

McGough and Burgoon (Ref. 24) showed a typical intensity distribution originating from the arc and corresponding filtering requirements. According to their work, the intensity of the arc light should be filtered to about 0.00027% of its original value (≅ 1/40,000) to be clearly seen. In order to block the small arc and filter the welding area gradually, an optical mask is used. The working principle of the optical mask with an axisymmetric lens is to reduce the light intensity at a location by placing an object that blocks at least part of the light source. The location of the optical mask, and hence the light intensity that reaches the camera, is adjusted by moving it back and forth, depending on the region to be filtered. This provides the required filtering of the arc light for the vision system to view the weld pool.

Details of the vision system are shown in Fig. 4, sketching the location of the CCD camera, optical lens, narrow-band-pass filter, protective lens, optical mask, and air hole for fume removal. Figure 5 shows the view obtained with this vision system, not yet mounted on the hood, using a Lincoln Electric Magnum 400 welding gun. The weld pool and its borders can now clearly be seen by the CCD camera, while this was not possible without the mask in place.

Final Design

Several hoods were designed and examined to see whether they satisfied the flow pattern requirements. Of these designs, the one that performed best for welding on a flat surface is shown in Fig. 6. Other hoods were designed for welding at 90-deg interior and exterior corners. All hoods had double walls through which the fumes were removed, providing radial flow around the arc so that the suction does not interfere with the flow of the shielding gas. The suction also provides cooling to the hood walls by drawing cool air from outside the hood. In order to keep the hood as light as possible, 0.08-in. mild steel sheet was used. All the hoods were built at Lehigh University.

The camera and illumination systems were placed together to allow the welder to see both sides of the weld interface (backward and forward). As discussed above, the system consists of a laser light source with a narrow-band-pass filter and an optical mask to eliminate the direct arc light to the miniature bullet CCD camera. To keep the screen of the vision system clean, a venting hole was drilled on the shielding gas nozzle. Figure 6 shows the schematic of the flat surface welding hood, while Fig. 7 shows the prototypes of the flat surface and the 90-deg interior corner hoods. Figure 7C and D shows the skids that were added to the corner hood to aid the welder in properly locating the hood since the weld is only seen through the camera. The disadvantage of not being able to directly view the welding area is compensated by the reduction or elimination of the UV exposure, spattering, noise, and welding fumes. Alternative designs may be possible to reduce the size of the corner hood.

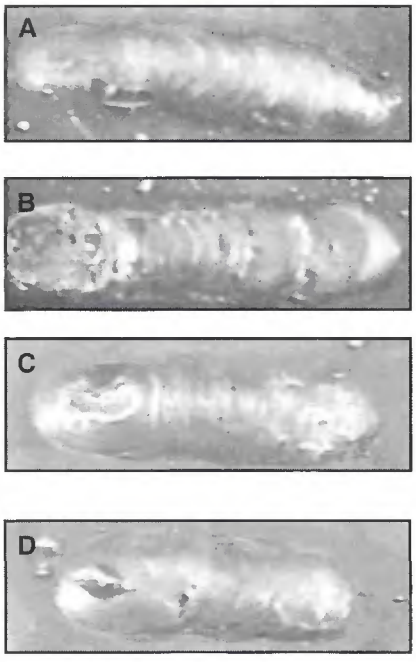

Fig. 10 — Comparison of welding quality with and without the lightweight welding hood. A — Without the hood, shielding gas of 11 ft³/h; B — without the hood, shielding gas of 9 ft³/h; C — with the hood, shielding gas of 5 ft³/h; D — with the hood, shielding gas of 3 ft³/h.

Experimental Setup

The hood was tested on a Lincoln Electric Powerwave 455 welding machine with 0.045-in. ER 70S-6 electrode. It was mounted on a Magnum 400 welding gun (by Lincoln Electric Co.). A high-vacuum Lincoln Electric X-Tractor 1GC was used as a suction device. The electrode wire speed was 100 in./min with constant arc voltage of 20 V, and a mixture of 75% Ar and 25% CO_2 was used as shielding gas. The volumetric flow of fume removed was measured using a rotameter and adjusted with a valve placed after it. The miniature bullet camera on the hood was connected to a display unit and a video recorder. Figure 8 shows the hood attached to the welding gun with the fume-removal and vision system in place, while Fig. 9 shows the weld area when the arc is on, and how the arc light also helps in viewing the welding area.

A set of experiments was performed by

varying the shielding gas and fume suction flow rates. It was possible to reduce the suction flow rates to very low levels, but, at this time, the cooling of the hood became a problem. Therefore, the suction flow rate was fixed at 2 ft^3/min (0.056 m^3/min) achieving good fume suction flow and hood temperature control.

Using the surface appearance as an approximate measure of the welding quality, Fig. 10A and B illustrate the effect of the shielding gas flow rate when no hood is used. Figure 10A shows that a shielding gas flow rate of 0.183 ft^3/min (0.0052 m^3/min) produces a clean, shiny surface, while a 0.15 ft^3/min (0.00425 m^3/min) flow was inadequate and left an unsatisfactory, pitted, irregular surface as is shown in Fig. 10B. A second experiment was made with the hood in place, a suction flow rate of 2 ft^3/min (0.056 m^3/min), and two different shielding gas rates. It was found that using a much lower shielding gas, 0.083 ft^3/min (0.00235 m^3/min), the welding quality was good when the hood was in place (Fig. 10C). Further reducing the shielding rate, however, deteriorated the weld quality as can be seen in Fig. 10D. It is speculated that the reduction in the shielding gas requirements is due to the structure of the gas flow that keeps the air away of the arc region. Finally, fume emissions were measured using a standard AWS welding hood. No measurable fume emissions to the surroundings were detected, showing the effectiveness of the hood since, under normal conditions, the fume emissions would be in the range of 0.5–0.7 g/min.

Conclusions

The hood captures fumes at the source and significantly reduces the required suction flow rates. As a result, the dimensions of the suction unit and the filter element are reduced, providing easy handling of the fume removal system. Suction flow rates can be reduced to only a few percent of normal suction rates in high-vacuum suction devices (2 vs. 50 ft^3/min) (0.0567 vs. 1.41 m^3/min) while still achieving complete fume removal.

Because the hood totally covers the weld pool, the weld pool is isolated from the surrounding atmosphere, restricting air entrance to the welding area. This reduces the consumption of the shielding gas flow rate up to 50%. Additionally, the hood also provides shielding against UV radiation and spark exposures. Therefore, there may be no need for a welding helmet, and the requirements for protective clothing are reduced. The hood also reduces the noise level of welding. The welding process can also be recorded for quality control purposes.

Acknowledgments

Support provided by ONR Grant No. N00014-99-0887 is greatly appreciated.

List of Symbols

b = characteristic width of the plume
c_p = specific heat of the fluid
d = diameter of the hot source
e_1, e_2 = constants defined in text
F_0 = buoyancy flux defined in Equation 1
g = gravitational acceleration
g' = buoyancy distribution given in Equation 3
Gr = Grashof number = $g\beta(T_0\text{-}T_\infty)d_0^3/\nu$
h = convective heat transfer coefficient at the hot source
k_1, k_2 = constants defined in text
m = total mass flux in the plume
Nu = Nusselt number = hd/k
Pr = Prandtl number = $cp\mu/k$
$Q_0 = \neq d^2h(T_0\text{-}T_\infty)/4$ = heat flow at $z = z_0$
r = radial distance in axisymmetric plume
T_∞ = Ambient temperature
T_0 = hot source temperature
w = vertical velocity
z = distance to plume point source
z_0 = height of hot source in plume model
x = particulate mass fraction

Greek Symbols

α = r/z at the plume boundary = plume angle
β = volumetric coefficient of thermal expansion
μ = viscosity
ν = kinematic viscosity
$\Delta\rho = \rho_\infty - \rho$
ρ = gas density
ρ_0 = hot gas density
ρ_∞ = gas density of surroundings

References

1. Sjogren, B. 1988. Effect of gasses and particles in welding and soldering. *Occupational Medicine: Principles and Practical Applications*. 2nd ed. Chicago Yearbook Medical Publishers, pp. 1053–1060.

2. Ebihara, I. 1988. Lung carcinoma among workers exposed to dust: I- Welders. *J. Labor Science* 64: 565–578.

3. Moulin, J. J., Wild, P., and Hguenoer, J. M., et al. 1993. Mortality study among mild steel and stainless steel welders. *Br. J. Ind. Med.* 50: 234–243.

4. The National Shipbuilding Research Program, 1999. Welding fume study — Final report. Report No.: NSRP 0525, N7-96-9.

5. Chute, D. O., and Christ, B. W. 2000. The national shipbuilding research program welding fume study. Ship Production Symposium, August 24, 25, Williamsburg, Va.

6. Mortazavi, S. B. 1997. Engineering control of occupational exposure the welding fume by process modification. *Welding in the World* 39(6): 297–303.

7. Lancaster, J. F. 1984. *The Physics of Welding*. Pergamon Press, London.

8. Rudell, B., Akselsson, K. R., and Berlin, M. H. 1998. Growth of welding aerosol particles in high relative humidity and particle deposition in the human respiratory airways. *Journal of Aerosol Science* 19(7): 1153–1156.

9. Torit, D. 1996. Costly maintenance reduced in welding fume removal. *Filtration and Separation*, March: 209.

10. *Lincoln Environmental Systems-Low Vacuum Solutions*. February 1999. The Lincoln Electric Co., E13.40.

11. *Lincoln Environmental Systems-High Vacuum Solutions*. November 1999. The Lincoln Electric Co., E13.10.

12. Block-Bolten, A., and Eagar, T. W. 1984. Metal vaporization from weld pools. *Metallurgical Transactions B* 15B: 461–469.

13. Hewitt, P. 1995. The particle distribution, density, and specific surface area of welding fumes from SMAW and GMAW mild and stainless steel consumables. *Am. Ind. Hyg. Assoc. J.* 56: 128–131.

14. George, W., Albert, L. R., and Tamanini, F. 1977. Turbulence measurements in axisymmetric buoyant plume. *Int. J. of Heat and Mass Transfer* 20: 1145–1154.

15. Malin, M. R. 1989. Analysis of turbulent forced plumes into a stable environments. *Appl. Math. Modeling* 13: 122–126.

16. Dewan, A., Arakeri, H. J., and Srinivasan, J. 1997. A new turbulence model for the axisymmetric plume. *Appl. Math. Modeling* 21: 709–719.

17. List, E. J. 1982. Turbulent jets and plumes. *Annual Review Fluid Mechanics* 48: 189–201.

18. Rouse, H., Yih, C. S., and Humphreys, W. H. 1952. Gravitational convection from a boundary surface. *Tellus* 4: 201.

19. Fishenden, M., and Saunders, O. A. 1950. *An Introduction to Heat Transfer*. Oxford, London.

20. Baum, H. R., and Mulholland, G. W. 1979. Coagulation of smoke aerosol in a buoyant plume. *J. of Colloid and Interface Science* 72(1): 1–12.

21. Albert, R. V. 1996. Fume Generation in Gas Metal Arc Welding. Ph.D. thesis, University of New Hampshire.

22. Allemand, C. D., Schoeder, R., Ries, D. E., and Eagar, T. W. 1985. A method of filming metal transfer in welding arcs. *Welding Journal* 64(1): 45.

23. Kovacevic, R., and Zhang, Y. M. 1995. Vision sensing of 3-D weld pool surface. *Proceedings of the 4th International Conference on Trends in Welding Research*. Gatlinburg, Tenn.

24. McGough, M. S., and Burgoon, C. 1990. Visual Monitoring of Remote Welding Operations. *Welding Journal* 69(12): 23.

25. Richardson, R.W., Gutow, D. A., Anderson, R. A., and Farson, D. F. 1984. Coaxial arc weld pool viewing for process monitoring and control. *Welding Journal* 63(3): 43.

26. Olander, L. 1986. Welding fume plumes in industrial workrooms. *Ventilation '85*, Elsevier, Amsterdam; New York, p. 153.